

Supplementary Materials

Metal-Site Dispersed Zinc-Chromium Oxide Derived from Chromate-Intercalated Layered Hydroxide for Highly Selective Propane Dehydrogenation

Lu Xue¹, Maoqi Pang¹, Zijian Yuan¹ and Daojin Zhou^{1,*}

1 State Key Laboratory of Chemical Resource Engineering, Beijing University of Chemical Technology, Bei-jing, China

* Correspondence: zhoudj@mail.buct.edu.cn

CONTENTS

Supplementary Materials.....	1
CONTENTS.....	2
Figure S1. TEM of (a) $\text{Zn}_1\text{Cr}_2\text{-CO}_3^{2-}$ and (b) $\text{Zn}_1\text{Cr}_2\text{-CrO}_4^{2-}$ precursors.....	3
Figure S2. Raman spectrum of the $\text{Zn}_1\text{Cr}_2\text{-CO}_3^{2-}$ and $\text{Zn}_1\text{Cr}_2\text{-CrO}_4^{2-}$ precursors.....	3
Figure S3. XPS spectra of Cr 2p over the $\text{Zn}_1\text{Cr}_2\text{-CrO}_4^{2-}$ precursor	3
Figure S4. XRD patterns of (a) different compositions of $\text{ZnCr-CrO}_4^{2-}\text{-MMO}$ and (b) $\text{Zn}_1\text{Cr}_2\text{-CrO}_4^{2-}$ calcined at different temperatures.	4
Figure S5. TEM of (a) $\text{Zn}_1\text{Cr}_2\text{-CO}_3^{2-}\text{-MMO}$ and (b) $\text{Zn}_1\text{Cr}_2\text{-CrO}_4^{2-}\text{-MMO}.$	4
Figure S6 (a) Initial propane conversion and (b) propylene selectivity of $\text{Mg}_2\text{Cr}_1\text{-CrO}_4^{2-}\text{-MMO}$, $\text{Zn}_1\text{Cr}_2\text{-CO}_3^{2-}\text{-MMO}$ and $\text{Zn}_1\text{Cr}_2\text{-CrO}_4^{2-}\text{-MMO}$ (Reaction conditions: 550 °C, WHSV = 22.3 h ⁻¹ , $\text{C}_3\text{H}_8\text{:N}_2 = 1:4.32)$	5
Figure S7. (a) Propane conversion and (b) propylene selectivity of $\text{Zn}_1\text{Cr}_2\text{-CO}_3^{2-}\text{-MMO}$ and $\text{Zn}_1\text{Cr}_2\text{-CrO}_4^{2-}\text{-MMO}$ (Reaction conditions: 550 °C, WHSV = 22.3 h ⁻¹ , $\text{C}_3\text{H}_8\text{:N}_2 = 1:4.32$). (c) Propane conversion and (d) propylene selectivity of $\text{Zn}_1\text{Cr}_2\text{-CrO}_4^{2-}\text{-MMO}$ with different WHSV.	5
Figure S8. (a) $\text{NH}_3\text{-TPD}$ and (b) Py-IR of different proposition $\text{ZnCr-CrO}_4^{2-}\text{-MMO}.$	6
Figure S9. XPS spectra of Cr 2p over $\text{Zn}_1\text{Cr}_2\text{-CO}_3^{2-}\text{-MMO}$ after reaction.	6
Figure S10. XRD patterns of $\text{Zn}_1\text{Cr}_2\text{-CO}_3^{2-}\text{-MMO}$ (a) and $\text{Zn}_1\text{Cr}_2\text{-CrO}_4^{2-}\text{-MMO}$ (b) after reaction.	6
Figure S11. TEM of $\text{Zn}_1\text{Cr}_2\text{-CO}_3^{2-}\text{-MMO}$ (a) and $\text{Zn}_1\text{Cr}_2\text{-CrO}_4^{2-}\text{-MMO}$ (b) after reaction.....	7
Figure S12. TGA of $\text{Zn}_1\text{Cr}_2\text{-CO}_3^{2-}\text{-MMO}$ and $\text{Zn}_1\text{Cr}_2\text{-CrO}_4^{2-}\text{-MMO}$ after reaction.	7
Table S1. Comparison of catalytic performance in this work with previous works.	8
Table S2. NH_3 desorption property of the catalysts.....	9

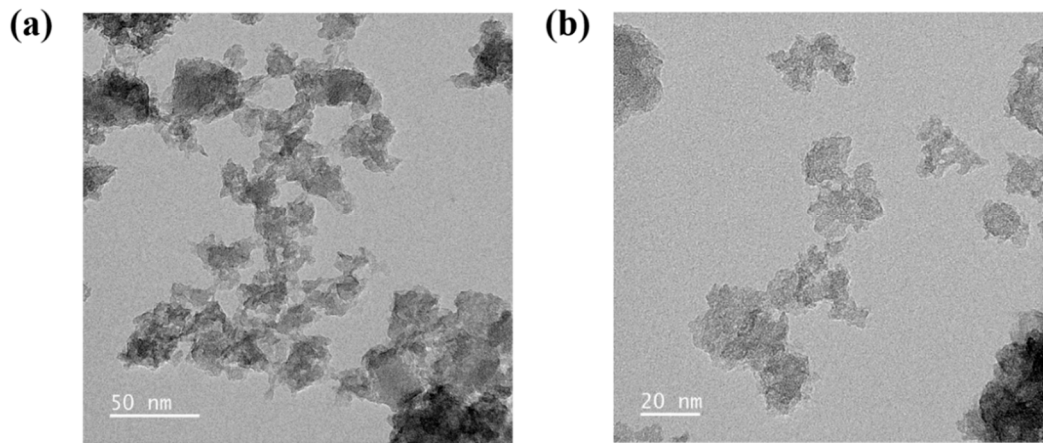


Figure S1. TEM of (a) $\text{Zn}_1\text{Cr}_2\text{-CO}_3^{2-}$ and (b) $\text{Zn}_1\text{Cr}_2\text{-CrO}_4^{2-}$ precursors.

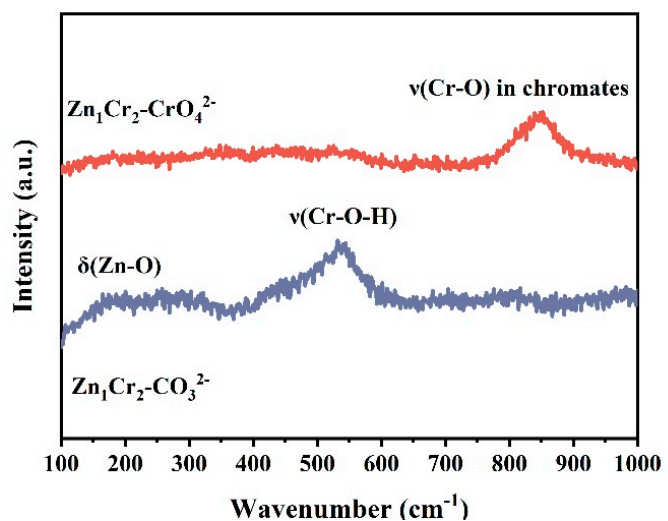


Figure S2. Raman spectrum of the $\text{Zn}_1\text{Cr}_2\text{-CO}_3^{2-}$ and $\text{Zn}_1\text{Cr}_2\text{-CrO}_4^{2-}$ precursors.

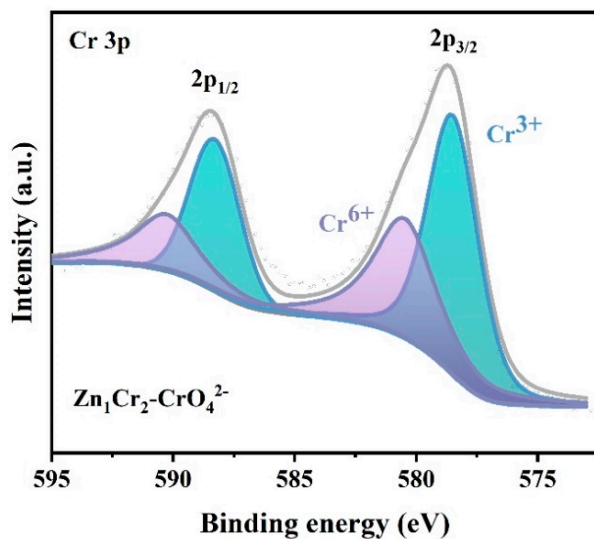


Figure S3. XPS spectra of Cr 2p over the $\text{Zn}_1\text{Cr}_2\text{-CrO}_4^{2-}$ precursor.

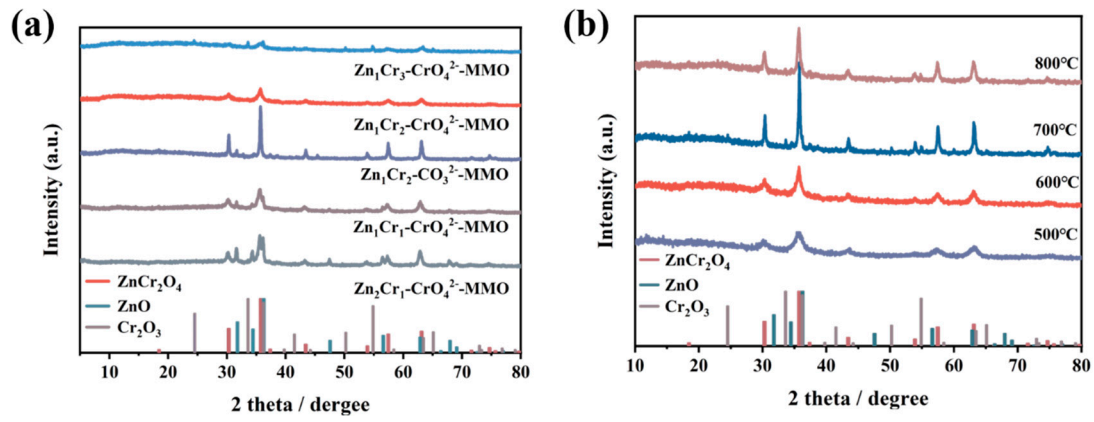


Figure S4. XRD patterns of (a) different compositions of $\text{ZnCr}-\text{CrO}_4^{2-}\text{-MMO}$ and (b) $\text{Zn}_1\text{Cr}_2\text{-CrO}_4^{2-}$ calcined at different temperatures.

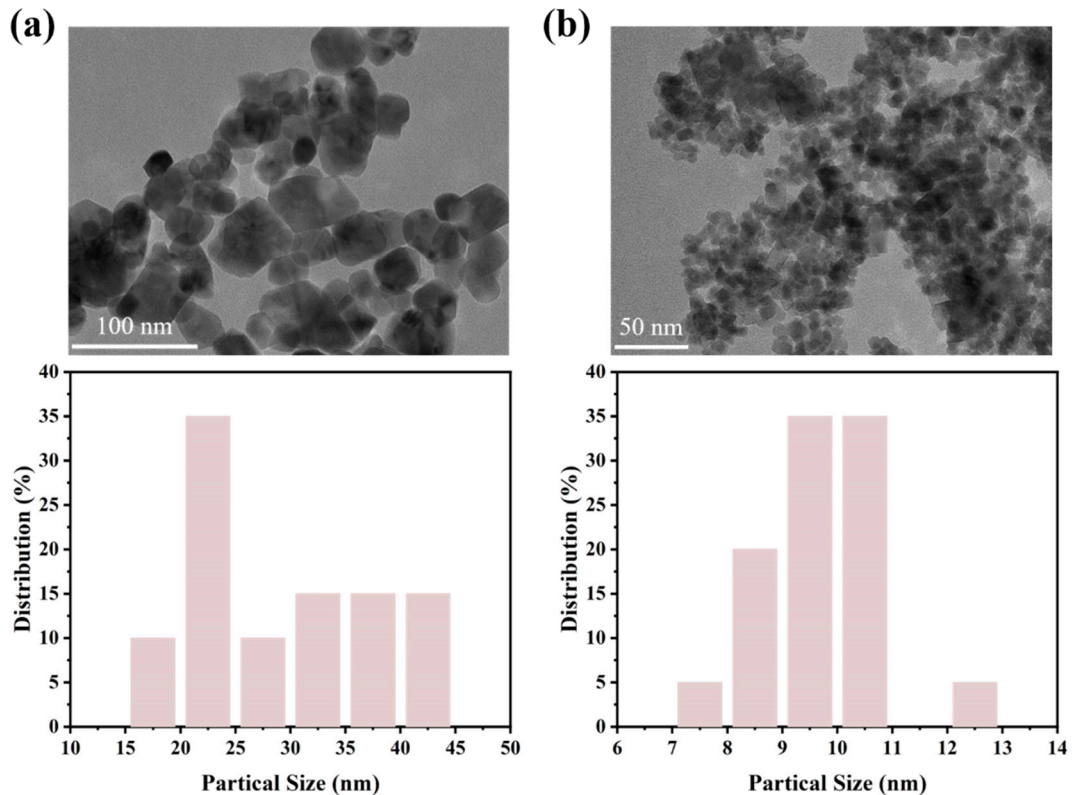


Figure S5. TEM of (a) $\text{Zn}_1\text{Cr}_2\text{-CO}_3^{2-}\text{-MMO}$ and (b) $\text{Zn}_1\text{Cr}_2\text{-CrO}_4^{2-}\text{-MMO}$.

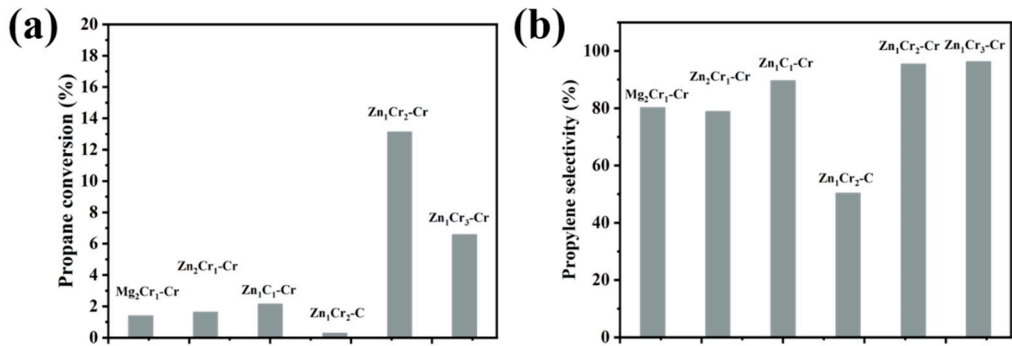


Figure S6 (a) Initial propane conversion and (b) propylene selectivity of Mg₂Cr₁-CrO₄²⁻-MMO, Zn₁Cr₂-CO₃²⁻-MMO and Zn₁Cr₂-CrO₄²⁻-MMO (Reaction conditions: 550 °C, WHSV = 22.3 h⁻¹, C₃H₈:N₂ = 1:4.32).

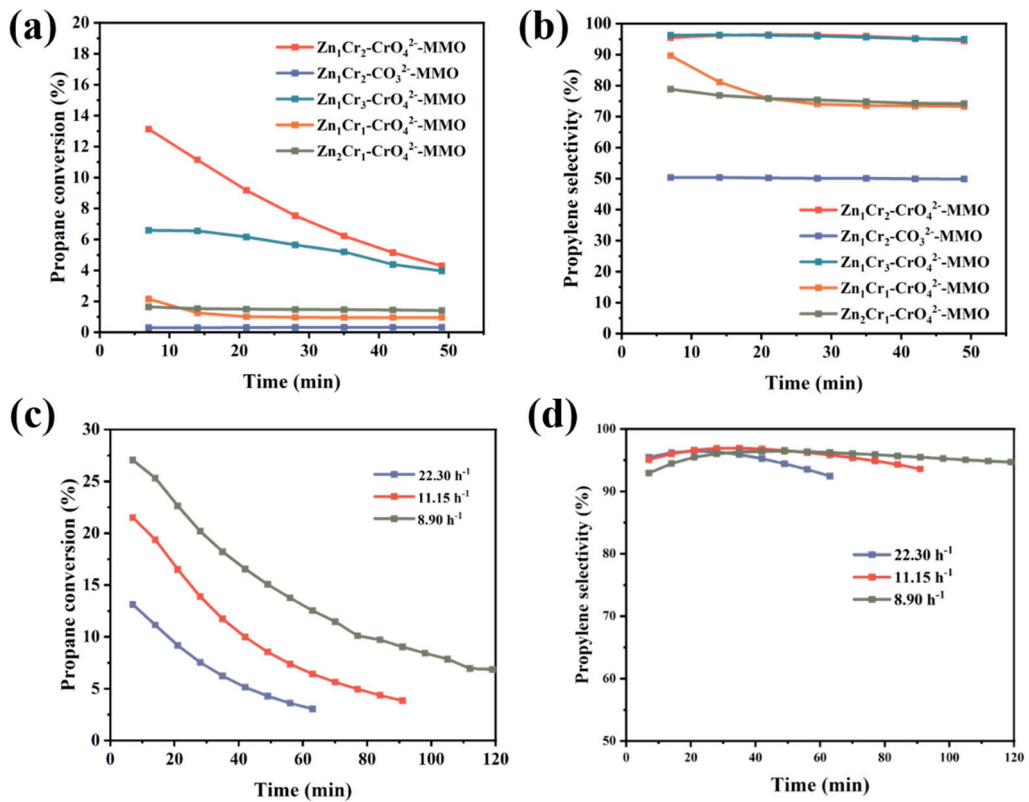


Figure S7. (a) Propane conversion and (b) propylene selectivity of Zn₁Cr₂-CO₃²⁻-MMO and Zn₁Cr₂-CrO₄²⁻-MMO (Reaction conditions: 550 °C, WHSV = 22.3 h⁻¹, C₃H₈:N₂ = 1:4.32). (c) Propane conversion and (d) propylene selectivity of Zn₁Cr₂-CrO₄²⁻-MMO with different WHSV.

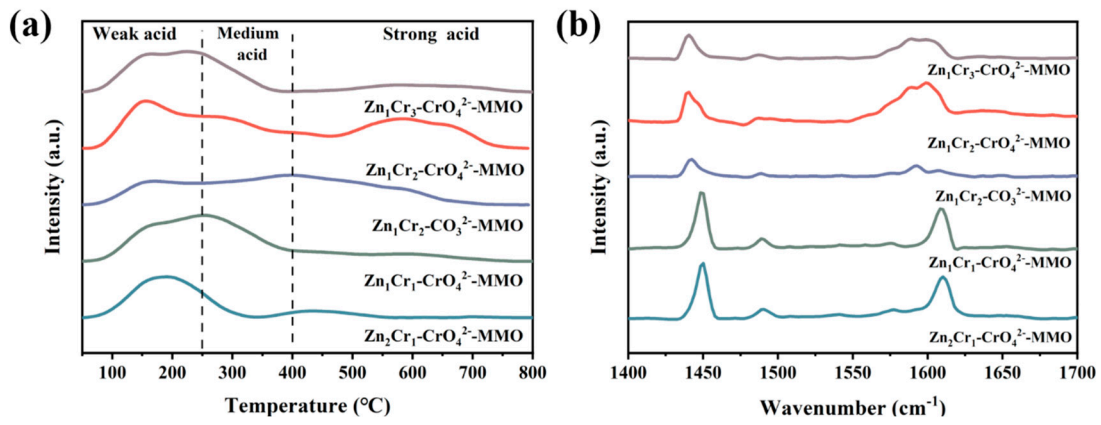


Figure S8. (a) NH₃-TPD and (b) Py-IR of different proposition ZnCr-CrO₄²⁻-MMO.

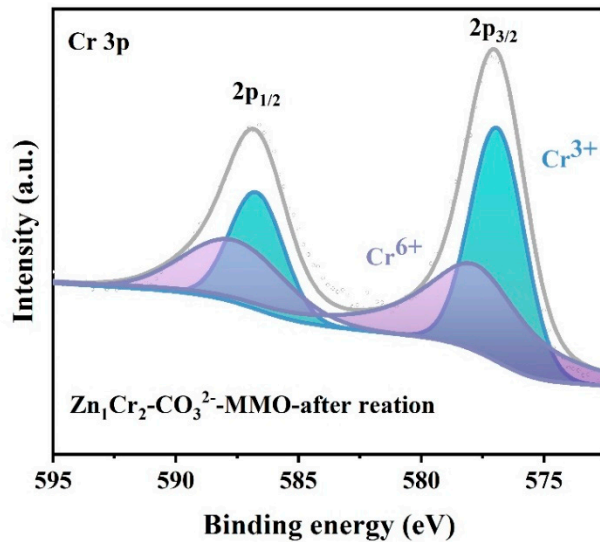


Figure S9. XPS spectra of Cr 2p over Zn₁Cr₂-CO₃²⁻-MMO after reaction.

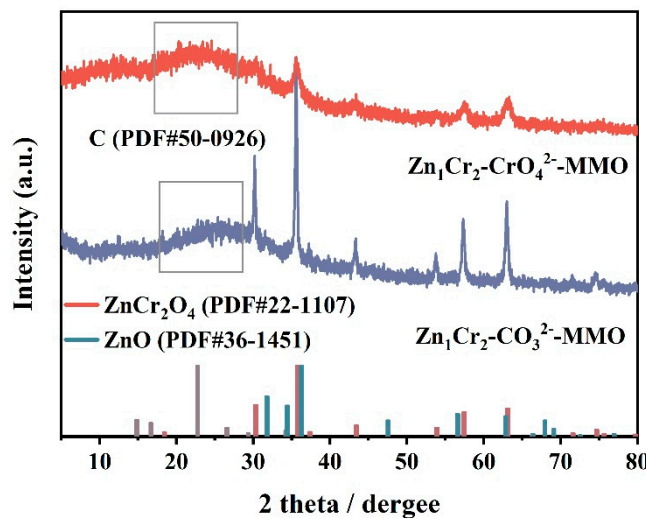


Figure S10. XRD patterns of Zn₁Cr₂-CO₃²⁻-MMO (a) and Zn₁Cr₂-CrO₄²⁻-MMO (b) after reaction.

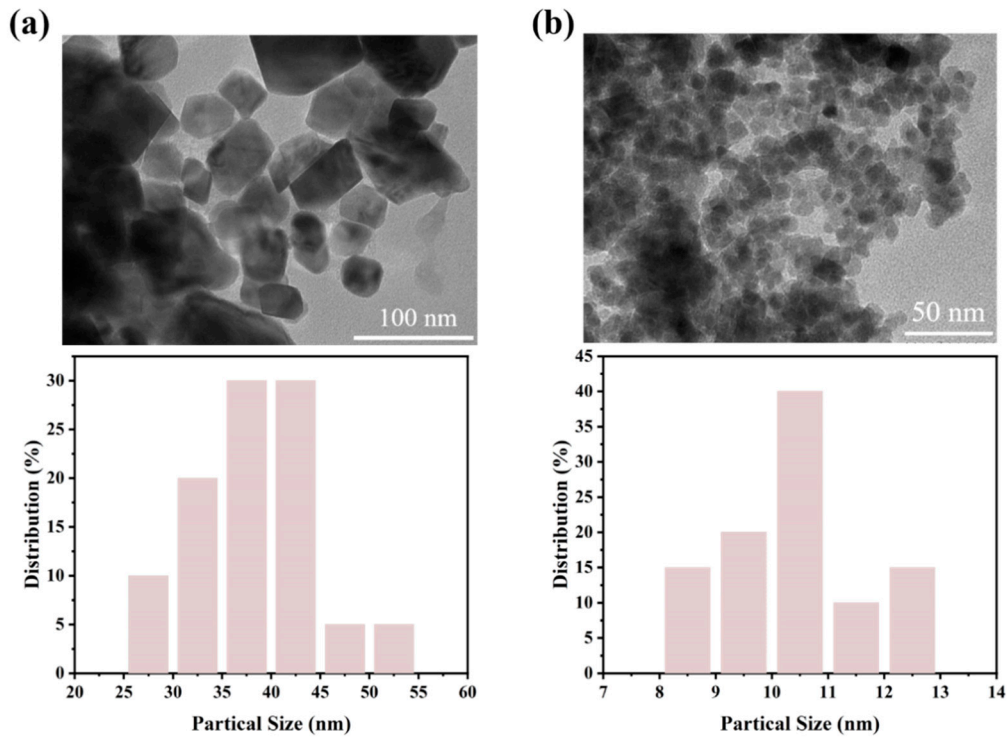


Figure S11. TEM of $\text{Zn}_1\text{Cr}_2\text{-CO}_3^{2-}\text{-MMO}$ (a) and $\text{Zn}_1\text{Cr}_2\text{-CrO}_4^{2-}\text{-MMO}$ (b) after reaction.

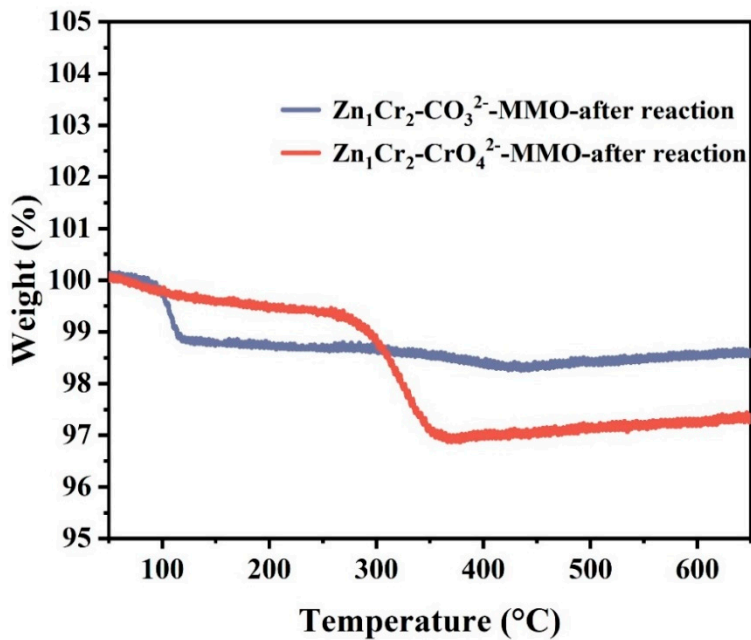


Figure S12. TGA of $\text{Zn}_1\text{Cr}_2\text{-CO}_3^{2-}\text{-MMO}$ and $\text{Zn}_1\text{Cr}_2\text{-CrO}_4^{2-}\text{-MMO}$ after reaction.

Table S1. Comparison of catalytic performance in this work with previous works.

Catalysis	Temperature(°C)	WHSV	Feed composition	Conversion (%)	Selectivity (%)	Ref
Co-Al ₂ O ₃	590	2.9h ⁻¹	C ₃ H ₈ :H ₂ :N ₂ =1:0.8:3.2	24.8	>97.1	[40]
0.5%Co@Si-BEA	590	3.66 h ⁻¹	C ₃ H ₈ :H ₂ :N ₂ =5:4:5	25	>93	[41]
Mo ₂ N	500	/	10 vol% C ₃ H ₈ in Ar	~11	95	[37]
Co SAs/SiO ₂ NM _s	550	2.9 h ⁻¹	C ₃ H ₈ : N ₂ = 2:6.4	25	95	[42]
Na-Sn-Beta-30	630	/	20 mol % C ₃ H ₈ /80 mol % N ₂	40	92	[38]
VO _x /Al ₂ O ₃	600	3 h ⁻¹	28 vol% C ₃ H ₈ , 28% H ₂ in N ₂	32	94	[43]
Cr-Al-800	600	/	/	33.2	90.4	[31]
Zn-4@S-1	600	2.4 h ⁻¹	10% C ₃ H ₈ balanced by He	41	97	[44]
Zn _{0.3} Cr	480	5000 ml h ⁻¹ gcat ⁻¹	C ₃ H ₈ :Ar = 5:95.	31.3	94	[45]
CrZrO _x /SiO ₂	550	34.5 h ⁻¹	40vol% C ₃ H ₈ in N ₂	30	85(C=30)	[46]
Rh0.5Sn3.0	600	10.8h ⁻¹	H ₂ :N ₂ :C ₃ H ₈ = 1:1:1	30.8	96.3	[47]
VO _x /ZrO ₂	550	2.07h ⁻¹	C ₃ H ₈ :N ₂ :H ₂ =7:36:7	~25	>80	[48]
CoO _x @NC/S-1	600	1.5h ⁻¹	C ₃ H ₈ :N ₂ = 5:19	40	>97	[49]
CrO _x /HZSM-5	/	0.59h ⁻¹	C ₃ H ₈ :N ₂ = 5:95	~32.6	~94.2	[32]
Zn ₁ Cr ₂ -Cr-MMO	550	8.9h ⁻¹	C ₃ H ₈ :N ₂ =1:4.32	27	>90	This work

Table S2. NH₃ desorption property of the catalysts.

Catalyst	Weak acid site (mmol/g)	Medium acid Site (mmol/g)	Strong acid site (mmol/g)	Total acid site (mmol/g)
Zn ₂ Cr ₁ -CrO ₄ ²⁻ - MMO	0.1847	0.0354	0.0295	0.2496
Zn ₁ Cr ₁ -CrO ₄ ²⁻ - MMO	0.1954	0.1662	0.0824	0.4440
Zn ₁ Cr ₂ -CO ₃ ²⁻ - MMO	0.1185	0.1450	0.1978	0.4613
Zn ₁ Cr ₂ -CrO ₄ ²⁻ - MMO	0.2157	0.1396	0.2503	0.6056
Zn ₁ Cr ₃ -CrO ₄ ²⁻ - MMO	0.2024	0.0880	0.0567	0.3471